Journal of Power Sources 182 (2008) 278–283

Contents lists available at ScienceDirect

Journal of Power Sources

journal homepage: www.elsevier.com/locate/jpowsour

Investigation of mechanical activation on Li–N–H systems using ^{6}Li magic angle spinning nuclear magnetic resonance at ultra-high field

Jian Zhi Hu[a,*], Ja Hun Kwak[a], Zhenguo Yang[a], William Osborn[b], Tippawan Markmaitree[b], Leon L. Shaw[b]

[a] *Pacific Northwest National Laboratory, 902 Battelle Boulevard, Richland, WA 99352, USA*
[b] *Department of Chemical, Materials and Biomolecular Engineering, University of Connecticut, Storrs, CT 06269, USA*

ARTICLE INFO

Article history:
Received 16 February 2008
Received in revised form 1 April 2008
Accepted 2 April 2008
Available online 10 April 2008

Keywords:
MAS NMR
^{6}Li
^{1}H
Mechanical activation
Hydrogen storage
Dynamics

ABSTRACT

The significantly enhanced spectral resolution in the ^{6}Li MAS NMR spectra of Li–N–H systems at ultra-high field of 21.1 T (corresponding to a proton Larmor frequency of 900 MHz) is exploited, for the first time, to study the detailed electronic and chemical environmental changes associated with mechanical activation (MA) of the Li–N–H system using high-energy balling milling. Complementary to ultra-high field studies, the hydrogen discharge dynamics are investigated using variable temperature *in situ* ^{1}H MAS NMR at 7.05 T field. It is shown that the changes in the ^{6}Li MAS spectra of LiH and $LiNH_2$ induced by MA can be separated from those of the LiOH and $LiOH{\bullet}H_2O$ impurities in the samples, and a new ^{6}Li peak induced by MA, which has never been reported before, is identified with the aid of the ultra-high field. The formation of this new peak and its associated upfield shift are attributed to the increased lattice defects induced by ball milling, which in turn enhances hydrogen release of the $LiH + LiNH_2$ mixture observed in the *in situ* study of the hydrogen discharge dynamics. The study also clearly indicates that ball milling at liquid nitrogen temperature produces more mechanical activation than ball milling at room temperature.

1. Introduction

In solid-state NMR, high spectral resolution requires the elimination or suppression of the various line broadenings arising from the anisotropic part of spin interactions so that a spectrum with sharp lines positioned at the isotropic chemical shifts is obtained. For nuclei with spin = 1/2 except protons that are strongly coupled by homonuclear dipolar interactions, high resolution can be obtained at usual magnetic fields using magic angle spinning (MAS) at conventional spinning rates combined with heteronuclear decoupling when necessary. For nuclei with $I = 3/2, 5/2, 7/2, \ldots$, the resonant peak is further broadened by the second-order perturbation of quadrupolar interaction that can not be eliminated by traditional MAS technique. For nuclei with $I = 1$ such as ^{6}Li, both first-order and small second-order interactions co-exist, where the first-order line broadening can be averaged out by MAS but second-order cannot. The second-order quadrupolar broadening expressed in ppm is proportional to the inverse square of Larmor frequency, or inversely proportional to the magnetic field strength when expressed in Hz. Consequently, a significant gain in both spectral resolution and sensitivity is expected at increasingly high magnetic fields [1].

The information of the electronic and chemical environment around nuclei obtained via NMR analysis is not easily accessible by the other analytical methods frequently used to quantify the effect of mechanical activation (MA), such as transmission electron microscopy (TEM), X-ray diffraction (XRD), differential scanning calorimetry (DSC), and Fourier transform infrared (FTIR) [2–4]. Thus, NMR is a valuable analytical tool complementary to TEM, XRD, DSC, and FTIR in quantifying the degree of MA obtained via high-energy ball milling. In our recent work [5], the effects of MA on potential hydrogen storage materials, i.e., the Li–N–H systems consisting of LiH and $LiNH_2$ [6–22], have been investigated using ^{1}H and ^{6}Li MAS NMR at a magnetic field of 7.05 T. It was found that the center of the ^{6}Li MAS peak shifted upfield with the use of high-energy ball milling in samples of $LiNH_2$ and $LiNH_2$ + LiH. The upfield shift has been attributed to the formation of defect structures. However, due to the limited spectral resolution at low magnetic field of 7.05 T, only one broad peak was observed for each of the samples, i.e., LiH, $LiNH_2$ and $LiNH_2$ + LiH mixture. Furthermore, the ^{6}Li NMR peak positions from these samples are very close, which seriously hamper the analysis of the spectrum.

In this work, the effects of high-energy ball milling are studied using ^{6}Li MAS NMR at ultra-high magnetic field. The high spectral

* Corresponding author. Tel.: +1 509 371 6544; fax: +1 509 376 6546.
E-mail address: Jianzhi.Hu@pnl.gov (J.Z. Hu).

0378-7753/$ – see front matter © 2008 Elsevier B.V. All rights reserved.
doi:10.1016/j.jpowsour.2008.04.007

resolution obtained at high field reveals detailed structural changes that are impossible to obtain at low magnetic field. Because of this high spectral resolution the changes in the ^{6}Li MAS spectra of LiH and $LiNH_2$ induced by MA can be separated from those of the LiOH and $LiOH^{\bullet}H_2O$ impurities in the samples, and a new ^{6}Li peak induced by MA, which has never been reported before, is identified. Furthermore, the effects of ball milling at liquid nitrogen temperature have been compared with that at room temperature using *in situ* variable temperature ^{1}H MAS NMR studies at 7.05 T field. The study clearly indicates that ball milling at liquid nitrogen temperature produces more mechanical activation than ball milling at room temperature.

2. Experimental

2.1. Sample preparation

Lithium amide ($LiNH_2$) with 95% purity was purchased from Alfa Aesar, while lithium hydride (LiH) with 95% purity was purchased from Sigma–Aldrich. The as-received $LiNH_2$ and LiH samples were used directly. The $LiNH_2$ and LiH mixture was prepared with a molar ratio of 1:1.1 according to the following reaction,

$$LiNH_2 + LiH = Li_2NH + H_2 \quad (1)$$

The 10% excess of LiH was added to minimize the loss of NH_3 during the dehydriding process. High-energy ball milling was conducted using a modified Szegvari attritor which had been shown previously to be effective in preventing the formation of the dead zone and producing uniform milling products within the powder charge [23]. Furthermore, a previous study has demonstrated that the seal of the canister of the attritor is air-tight and there is no oxidation during ball milling of LiH [24]. The canister of the attritor and balls with 6.4 mm in diameter were both made of stainless steels. The loading of balls and the powder to the canister was performed in a glovebox filled with ultra-high purity argon that contains Ar 99.999%, $H_2O < 1$ ppm, $O_2 < 1$ ppm, $H_2 < 3$ ppm, and $N_2 < 5$ ppm (referred to as Ar of 99.999% purity hereafter). The ball-to-powder weight ratio was 60:1, the milling speed was 600 rpm, and the milling temperature was maintained either at 20 °C (room temperature), achieved by water cooling at a flowing rate of 770 ml min^{-1}, or at liquid nitrogen (LN_2) temperature. For liquid nitrogen (LN_2) milling, the milling vessel was cooled to LN_2 temperature (−196 °C) before the milling started and maintained at LN_2 temperature during the milling. Ball milling time was a variable in this study and adjusted from 45 to 180 min. The samples were stored in a dry argon glovebox until NMR measurements and loaded into sealed NMR rotors while inside the glovebox to avoid exposing to air.

Two identical samples of $LiNH_2$ + LiH were prepared using LN_2 mill for 180 min. One of them named as "$LiNH_2$ + LiH-LN_2-as-mill" refers to the milled sample directly from the mill vessel, while the other one named as "$LiNH_2$ + LiH-LN_2-mill-post-10cycles" indicates the fully desorbed sample after 10 charge and discharge cycles at 285 °C, followed by a full desorption procedure typically used for determining the pressure-composition isotherm at 285 °C [25]. The charge segment in the 10 charge/discharge cycles entailed 1 h holding under 10 bar of hydrogen pressure, whereas the discharge segment was 2.5 h holding under an evacuated condition with a hydrogen pressure of ∼0.03 bar, both at 285 °C. Both charge/discharge cycles and the subsequent full desorption via the pressure-composition isotherm procedure were performed using a Sieverts'-type pressure-composition-isotherm (PCI) device (Advanced Materials Corporation). Given the last step of the full desorption, lithium imide (Li_2NH) should be the dominant phase in the sample labeled with "$LiNH_2$ + LiH-LN_2-mill-post-10cycles" as indicated by Eq. (1). All other samples not labeled by "LN_2" refer to the samples ball milled at room temperature.

2.2. NMR experiment

The ultra-high field ^{6}Li MAS NMR experiments were performed on a Varian-Oxford Inova 63 mm widebore 900 MHz NMR spectrometer. The main magnetic field was 21.1 T and the corresponding ^{6}Li Larmor frequency was 132.531 MHz. A home-made 3.2 mm pencil-type MAS probe was used for the ^{6}Li NMR experiments. About 5–8 mg of samples was used for each measurement and a sample-spinning rate of about 18 kHz was used. A Bloch decay pulse sequence was used for the measurement with the recycle delay time as 70 s and the number of scans varied between 5 and 847, depending on the sensitivity of the sample. All the ultra-high field ^{6}Li MAS spectra were acquired at room temperature and were referenced to 1 M LiCl in H_2O (0 ppm).

The low-field ^{6}Li MAS and in situ variable temperature ^{1}H MAS experiments were performed on a Varian-Chemagnetics 300 MHz Infinity spectrometer, corresponding to ^{1}H and ^{6}Li Larmor frequencies of 299.982 and 44.146 MHz, respectively. A commercial cross-polarization/MAS probe with a 7.5 mm outside diameter and 6 mm internal diameter pencil-type spinner system was used. The sample cell resembles the commercial cell except that two solid Teflon plugs were made in such a manner that they can only be fully inserted into the zirconium cylinder after being soaked in liquid nitrogen to seal ∼0.1 to 0.2 g of samples for variable temperature studies. The sample was first spun to the targeted spinning rate, i.e., 5.0 kHz ± 2 Hz using a commercial Chemagnetics MAS speed controller prior to raising the temperature. The ^{6}Li MAS experiments were performed at room temperature and 1 M LiCl in H_2O was used as the reference. Each spectrum was acquired using a single pulse excitation sequence (∼30° pulse width) with high power ^{1}H decoupling and a recycle delay time of 100 s. In the case of ^{1}H MAS (5.0 kHz) NMR, tetrakis(trimethylsilyl) silane (TKS), $[(CH_3)_3Si]_4Si$, was used as the reference, and spectra were acquired using a single 20° pulse excitation and a recycle delay time of 1 s.

3. Results and discussion

3.1. Resolution enhancement at ultra-high magnetic field in ^{6}Li MAS experiments

The advantages of ultra-high field are illustrated in Fig. 1, where the ^{6}Li MAS spectra acquired on a solid powder sample of LiH at magnetic fields of 7.05 T (300 MHz) and 21.1 T (900 MHz) are presented. It follows from Fig. 1 that only a single peak with approximately a Gaussian lineshape is obtained on the 300 MHz spectrometer (top trace). The linewidth ($\delta\upsilon_{1/2}$), defined as the full linewidth at half peak height positions, is 4.75 ppm, or 210 Hz. However, three peaks are unambiguously observed on the 900 MHz spectrum (bottom trace), consisting of two well-resolved major peaks, labeled as "1" at about 0.0 ppm for $LiOH^{\bullet}H_2O$, "3" at about 2.7 ppm for LiH, and a low intensity shoulder peak labeled as "2" at 1.1 ppm for LiOH. The assignments of these peaks are based on Fig. 2 that will be discussed shortly. Note that the assignment of the $LiOH^{\bullet}H_2O$ peak is also consistent with a previous report by Meyer et al. [26], where the center of the ^{7}Li MAS peak for $LiOH^{\bullet}H_2O$ was at about 0.4 ppm on a 700 MHz NMR spectrometer. It is known from the bottom trace in Fig. 1 that the linewidth for the LiH peak is 0.66 ppm, or 87.2 Hz. The experimental linewidth in unit of Hz, i.e., 210 Hz at 300 MHz and 87.2 Hz at 900 MHz, is approximately inversely proportional to the strength of the magnetic field, indicating that the major contribution to the linewidth in ^{6}Li MAS

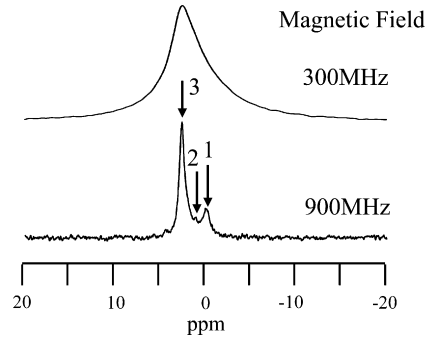

Fig. 1. ^{6}Li MAS NMR spectra of solid powder LiH sample that was ball milled for 45 min at room temperature. Top trace: acquired on a 300 MHz NMR spectrometer using about 200 mg of sample at a sample-spinning rate of 5 kHz ($\delta\upsilon_{1/2}$ = 4.75 ppm, or 210 Hz). The spectrum was featureless. Bottom trace: acquired on a 900 MHz spectrometer using about 5 mg of sample and at a sample-spinning rate of 18 kHz. Three well-resolved resonances corresponding to distinct chemical environments, i.e., LiOH•H_2O (peak 1), LiOH (peak 2), and LiH (peak 3, $\delta\upsilon_{1/2}$ = 0.66 ppm, or 87.2 Hz), were obtained. Both spectra were acquired using a single pulse sequence with the recycle delay time/scans as 100 s/1024 scans (top) and 70 s/400 scans (bottom), respectively.

experiment is from the second-order quadrupolar line broadening. The significantly enhanced spectral resolution at ultra-high field of 900 MHz relative to 300 MHz arises from the fact that ^{6}Li has a small quadrupole moment [27]. Therefore, the second-order broadening approaches zero at ultra-high magnetic field and an essentially high-resolution isotropic chemical shift is obtained at 900 MHz. This, combined with the fact that the isotropic chemical shift is proportional to the magnetic field in unit of Hz, generates a high-resolution ^{6}Li MAS spectrum at ultra-high magnetic field.

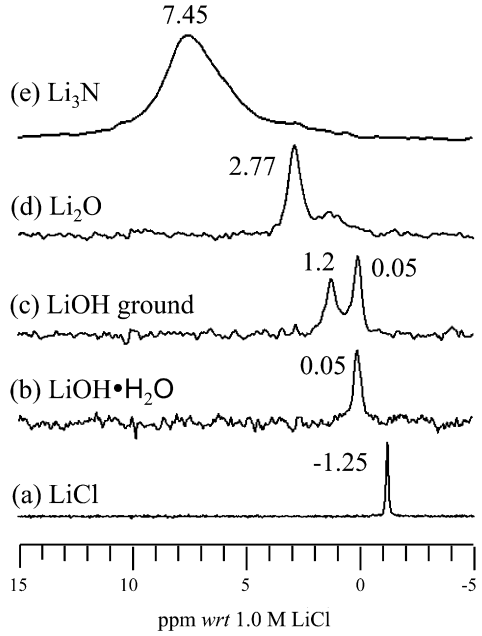

Fig. 2. ^{6}Li MAS NMR spectra of standard solid powder samples purchased from Aldrich. All the spectra were acquired on the 900 MHz NMR spectrometer and at a sample-spinning rate of 18 kHz. Approximately 5 mg of samples were used in each measurement. All the spectra were acquired using a single pulse (90° pulse angle) sequence with a recycle delay time of 70 s. The number of accumulations and the linewidth are: (a) solid LiCl, 78 scans, $\delta\upsilon_{1/2}$ = 17 Hz with 0 Hz line broadening; (b) LiOH•H_2O, 84 scans, $\delta\upsilon_{1/2}$ = 59 Hz with 20 Hz line broadening; (c) LiOH, 847 scans, $\delta\upsilon_{1/2}$ = 66 Hz (1.2 ppm) and 52 Hz (0.05 ppm) with 10 Hz line broadening; (d) Li_2O, 122 scans, $\delta\upsilon_{1/2}$ = 106 Hz with 35 Hz line broadening; and (e) Li_3N, 5 scans, $\delta\upsilon_{1/2}$ = 400 Hz with 20 Hz line broadening.

In additional to the spectral resolution enhancement at ultra-high magnetic field, the sensitivity is also dramatically enhanced. It is well known that if the linewidth remains constant at different magnetic fields, the NMR sensitivity is proportional to $B_0^{3/2}$, where B_0 is the external magnetic field strength. Given the fact that the second-order line broadening in unit of Hz is inversely proportional to B_0, the sensitivity of MAS experiment for quadrupolar nuclei would be proportional to $B_0^{5/2}$. Thus, the sensitivity at 900 MHz NMR spectrometer (21.1 T) would be approximately 15.58 times that obtained on a 300 MHz (7.05 T) spectrometer per unit weight of sample. Consequently, to acquire a spectrum using unit weight of sample with similar sensitivity the time needed at 900 MHz will only be about 0.41% of that at 300 MHz since sensitivity is proportional to the square root of the number of scans, or the square root of the total experimental time. Therefore, considerably smaller sample volume can be measured at 900 MHz than that at 300 MHz as sensitivity is also jointly proportional to the square root of the sample volume.

Fig. 2 summarizes the ultra-high field ^{6}Li MAS spectra acquired on several standard solid powder samples. With reference to 1 M LiCl in H_2O (0.0 ppm), the peak of solid LiCl (Fig. 2a) is located at −1.25 ppm with a half linewidth ($\delta\upsilon_{1/2}$) of only 17 Hz. Fig. 2b shows the spectrum of LiOH•H_2O sample that was prepared by first grinding the as-received LiOH sample (Aldrich) and then adsorbing saturated H_2O vapor into the sample for about 1 day at room temperature. A single peak is observed at about 0.05 ppm. Fig. 2c shows the spectrum of the as-received LiOH sample that was ground right before loading to the NMR rotor. Two peaks located at 0.05 and 1.2 ppm are observed. Based on the result from Fig. 2b, the 0.05 ppm is assigned to LiOH•H_2O, while the 1.2 ppm peak is attributed to LiOH. It is known from Fig. 2d that the peak position of Li_2O is at about 2.77 ppm. A lower shoulder peak centered about 1.2 ppm is also observed, indicating the existence of a small amount of LiOH in this sample. This is because when Li_2O is exposed to air, a small portion of Li_2O is reacting with H_2O to form LiOH. The resonant peak of Li_3N is found at 7.45 ppm (Fig. 2e). It is interesting to find that the half linewidth of the peak is increased significantly from Li_2O to Li_3N, presumably due to the significantly increased Li-ion conductivity in the Li_3N sample. It is known that Li_3N is a very fast Li-ion conducting material [28].

3.2. The effects of high-energy ball milling revealed by ^{6}Li MAS at ultra-high field

Fig. 3 shows the ^{6}Li MAS NMR spectra obtained on the 900 MHz NMR spectrometer and at a sample-spinning rate of 18 kHz. Fig. 3a is the spectrum for the as-purchased $LiNH_2$ sample, consisting of a major peak centered at about 2.6 ppm and a shoulder at about 1.4 ppm. The major peak at ~2.6 ppm is attributed to the crystallite $LiNH_2$ molecules. It should be pointed out that solid $LiNH_2$ is really an extended ionic solid with discrete Li^+ cations and NH_2^- anions. To simplify our discussion, the unit of $Li^+NH_2^-$ is called as a molecule in this work. The same terminology also applies to solid LiH. Note that in our previous low-field (7.05 T) studies [5], the center of the ^{6}Li MAS NMR peak for the as-purchased $LiNH_2$ sample was at approximately 1.89 ppm. This difference is attributed to the complex second-order quadrupole line broadening at low magnetic field, where the corresponding peaks, i.e., 2.6 and 1.4 ppm at ultra-high field, are severely broadened and overlapped at low field. As a result, the center of the peak appears at 1.89 ppm. It is hypothesized that the peak at 1.4 ppm in Fig. 3a is caused by $LiNH_2$ molecules that are interacting with H_2O. To validate this hypothesis, a ^{6}Li MAS spectrum (Fig. 3(a1)) was acquired on the $LiNH_2$ sample that was prepared by first grinding the as-received $LiNH_2$ sample

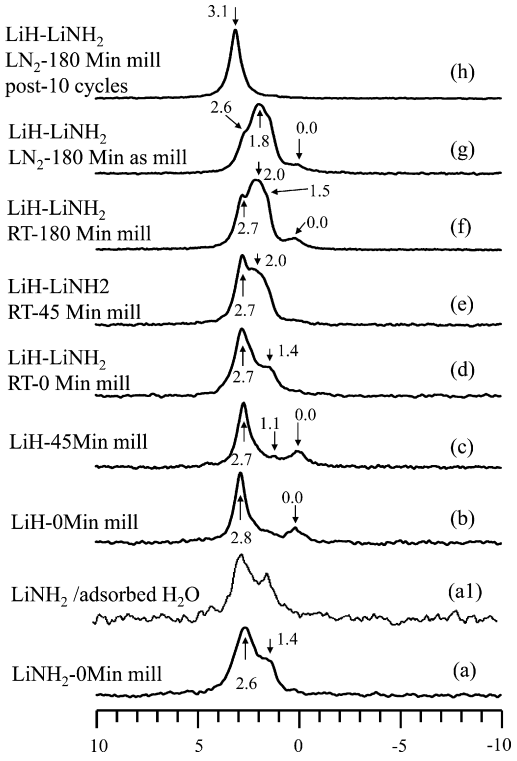

Fig. 3. ^{6}Li MAS spectra acquired with ultra-high magnetic field of 21.1 T (i.e., the 900-MHz NMR spectrometer) and at a sample-spinning rate of about 18 kHz. The amount of samples used for acquiring each spectrum was between 5 and 8 mg.

and then adsorbing saturated H_2O vapor into the sample for about 3 h at room temperature. It follows from Fig. 3(a1) that the peak at about 1.4 ppm is indeed increased, proving that the 1.4 ppm peak in Fig. 3a is from the $LiNH_2$ molecules that are interacting with H_2O. Furthermore, based on Fig. 2c, it can be inferred that the 1.4 ppm peak contains a substantial portion of the ^{6}Li MAS spectrum from LiOH.

Fig. 3b is the spectrum of the as-purchased LiH powder, while Fig. 3c is the spectrum of LiH that was ball milled at room temperature for 45 min. The presence of a small amount of LiOH (~1.1 ppm) and LiOH•H_2O (~0.0 ppm) in the as-purchased LiH powder is clearly visible, which is consistent with the previous XRD analysis [2]. The presence of a small amount of Li_2O in the as-purchased LiH is also likely; however, it cannot be confirmed under the present condition because of the overlap of Li_2O (2.77 ppm) and LiH (2.8 ppm) peaks. By comparing Fig. 3b with c, it is clear that the major peak corresponding to LiH (2.8 ppm) in the as-purchased LiH sample is upfield shifted to 2.7 in the sample ball milled at room temperature for 45 min. The upfield shift indicates changes in the average local electronic structure around Li nuclei, induced by MA through ball milling. Such a change is most likely due to the defect structure change within the hydride and amide particles induced by MA [5]. This hypothesis is further supported by results obtained from liquid nitrogen ball milled samples and will be discussed shortly. It should be pointed out that in our previous low-field (7.05 T) studies [5], the center of the peak for the as-purchased LiH sample was at about 2.50 ppm instead of the 2.81 ppm at ultra-high field. This is again due to the complex line broadening of LiH, LiOH and LiOH•H_2O in the sample from the second-order quadrupolar interaction at low magnetic field.

Fig. 3d is the spectrum of $LiNH_2$ + LiH without ball milling. It is clear that Fig. 3d is a simple superposition of a and b with the major peak centered at about 2.7 ppm. A major portion of the 2.7 ppm peak comes from the LiH. This is because in the mixture the ratio of LiH to $LiNH_2$ is 1.1:1.0. Also, the 2.8 ppm LiH peak in Fig. 3b is the dominant peak. Fig. 3e is the spectrum of $LiNH_2$ + LiH ball milled at room temperature for 45 min. The effects of ball milling in this mixed sample are the development of a relative broad peak centered at about 2.0 ppm and the shrinkage of the main peak at 2.7 ppm. It is also noted that the peak at 2.7 ppm in Fig. 3e is slightly narrower than its corresponding peak (2.7 ppm) in Fig. 3d. With an increase in the ball milling time to 180 min (Fig. 3f), the intensity of the peak at 2.7 ppm is further reduced while the intensity of the peak at about 2.0 ppm is significantly increased. In addition, a shoulder peak at about 1.5 ppm becomes visible, and the LiOH•H_2O peak at about 0.0 ppm is clearly observed. Note that the 2.0 ppm peak formed in the ball milled LiH + $LiNH_2$ mixture cannot be assigned to Li_2O, LiOH, and LiOH•H_2O (see Fig. 2), nor can it be attributed to the defect structure change within the LiH and $LiNH_2$ particles because ball milling of LiH alone does not lead to the appearance of this 2.0 ppm peak, but only the upfield shift of the LiH peak (Fig. 3c). Furthermore, this 2.0 ppm peak cannot be assigned to Li_2NH either. Li_2NH is the solid product from the chemical reaction between $LiNH_2$ and LiH if they react according to Eq. (1). As will be shown later, the ^{6}Li peak for Li_2NH is at 3.1 ppm. Thus, based on these observations, we postulate that high-energy ball milling of the $LiNH_2$ + LiH mixture has changed the defect structure within the $LiNH_2$ and LiH particles as well as induced molecular interactions between $LiNH_2$ and LiH particles. The former results in the upfield shift of the 2.7 ppm peak, whereas the latter leads to the formation of the 2.0 ppm peak. Furthermore, the nature of the molecular interactions between $LiNH_2$ and LiH particles is most likely related to the formation of a large amount of lattice defects on the surface of $LiNH_2$ and LiH particles, instead of the chemical reaction between $LiNH_2$ and LiH particles to form Li_2NH. The decreased intensity of the 2.7 ppm peak accompanied with the increased intensity of the 2.0 ppm peak as the degree of mechanical activation increases (i.e., from 0-min ball milling to 45-min and then to 180-min ball milling at room temperature) is consistent with the expectation that more Li atoms are changed to the surface state as the $LiNH_2$ and LiH particles become smaller with an increase in the degree of mechanical activation. This proposition is also consistent with the results obtained from liquid nitrogen ball milling to be discussed below.

Fig. 3g gives the ^{6}Li MAS spectrum of $LiNH_2$ + LiH ball milled at liquid nitrogen temperature for 180 min. By comparing with the 180-min room temperature milled results (Fig. 3f), two important observations can be obtained. First, the corresponding peaks in the liquid nitrogen milled sample are further shifted upfield by about 0.1–0.2 ppm (i.e., the 2.7 ppm peak in Fig. 3f is upfield shifted to 2.6 ppm in Fig. 3g, and the 2.0 ppm peak in Fig. 3f is shifted to 1.8 ppm in Fig. 3g), indicating that a larger change in the local electronic structure around Li nuclei for the liquid nitrogen ball milled sample than for the room temperature ball milled sample. Indeed, our previous study has shown that as the milling time at room temperature increases from 90 min to 180 min, the upfield shift increases [5]. The present study indicates that the upfield shift can be further increased by ball milling at liquid nitrogen temperature. Second, the linewidth corresponding to the dominant peak at about 1.8 ppm is slightly narrower than its counterpart in the room temperature milled sample (Fig. 3f), indicating a more uniform structure or a well-defined interaction between LiH and $LiNH_2$ molecules is formed by liquid nitrogen ball milling. Accompanied with the sharpening of the 1.8 ppm peak, the intensity of the peak at about 2.6 ppm is dramatically reduced in the liquid nitrogen ball milled sample. These phenomena are due to the stronger molecular interactions between $LiNH_2$ and LiH as well as more Li atoms changing to the surface state during ball milling at liquid nitro-

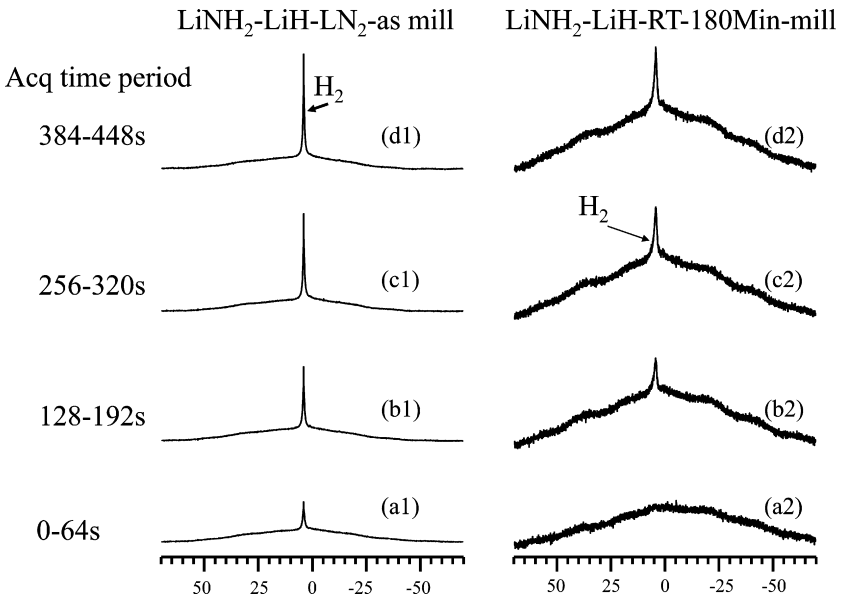

Fig. 4. ^{1}H MAS (5 kHz) NMR spectra as a function of time during the temperature ramp from room temperature to 180 °C. These spectra were acquired at a magnetic field of 7.05 T (300 MHz spectrometer). Each spectrum was acquired using 32 accumulation numbers and a total acquisition time of 64 s. Spectra (a1)–(d1) were acquired on 172 mg sample of $LiNH_2$ + LiH ball milled at liquid nitrogen temperature for 180 min. The integral ratios of H_2 peak at 4.08 ppm to the total spectrum and the associated half linewidths ($\delta\upsilon_{1/2}$) of the peaks are 6.7%, ~215 Hz for (a1), 13.98%, ~168 Hz for (b1), 17.5%, ~150 Hz for (c1), and 19.2%, ~130 Hz for (d1). Spectra (a2)–(d2) were obtained on 125 mg sample of $LiNH_2$ + LiH ball milled at room temperature for 180 min. The integral ratios of H_2 peak at 4.08 ppm to the total spectrum are ~0.1%, ~400 Hz for (a2), 2.3%, 400 Hz for (b2), 3.5%, 360 Hz for (c2), and 4.1%, 340 Hz for (d2). Note that in each spectral series, the spectra acquired during time periods of 64–128 s, 192–256 s, and 320–384 s are omitted in the plotting.

gen temperature than ball milling at room temperature. Thus, ball milling at liquid nitrogen temperature is more effective in mechanical activation than ball milling at room temperature, as evidenced by the upfield shift and decreased intensity of the 2.7 ppm peak accompanied with the increased intensity of the 1.8 ppm peak.

Fig. 3h shows the ^{6}Li MAS spectrum of $LiNH_2$ + LiH that was ball milled for 180 min at liquid nitrogen temperature, and subsequently subjected to 10 charge and discharge cycles followed by a complete desorption treatment at 285 °C. According to Eq. (1), Li_2NH should be the dominant structure associated with this fully discharged sample. Therefore, it is concluded that the peak position for Li_2NH is located at about 3.1 ppm. The nearly ideal symmetrical line shape in Fig. 3h indicates that Li_2NH is indeed the only dominant structure remaining in this fully desorbed sample.

3.3. *Probing the hydrogen discharge dynamics by in situ variable temperature ^{1}H MAS NMR*

In Fig. 4, ^{1}H MAS spectra of the samples, i.e., $LiNH_2$ + LiH-LN_2-as-mill (left column spectral traces) and $LiNH_2$ + LiH-RT-180Min-mill (right column spectral traces), as a function of heating time were compared. These spectra were acquired at a sample-spinning rate of 5 kHz and at a magnetic field of 7.05 T. For acquiring the spectra of each sample, at time zero, the temperature control unit was turned on and the temperature started to ramp to the targeted temperature of 180 °C during a time period of about 180 s. It was noticed that the first spectrum of each sample, i.e., Fig. 4(a1) for the $LiNH_2$ + LiH-LN_2-as-mill sample, or Fig. 4(a2) for the $LiNH_2$ + LiH-RT-180Min-mill, was acquired between the temperature of 25 and 100 °C, while the second spectrum of each sample, Fig. 4(b1) and (b2), was acquired between 160 and 180 °C. The third and the fourth spectra of each sample, Fig. 4(c1), (d1), (c2) and (d2), were acquired at 180 °C. In general, each spectral trace in Fig. 4 consists of two major peaks, i.e., a narrow peak located at about 4.1 ppm and a very broad peak underneath the narrow peak. The linewidth ($\Delta\upsilon_{1/2}$), obtained by measuring the full width at the half peak height positions, is approximately 20 kHz for the broad peak for all of the spectral traces in Fig. 4. The broad peak is generated by the rigid lattice protons, where proton homonuclear dipolar coupling is very strong and line narrowing by 5.5 kHz MAS is very inefficient and consequently a broad line is observed. On the other hand, the narrow peak at 4.1 ppm corresponds to both the gaseous and the chemical and physical adsorbed molecules, where the homonuclear dipolar coupling is averaged out in the case of free gaseous molecules due to fast random molecular motion or is significantly suppressed in the case of surface adsorbed molecules. As a result, a narrow peak is observed in the 5.5 kHz MAS spectrum. It is known from Fig. 4 that the linewidth of the 4.1 ppm peak decreases from ~215 Hz (Fig. 4(a1)) to ~150 Hz (Fig. 4(d1)), indicating a significantly increased amount of gaseous molecules is generated in the $LiNH_2$-LiH-LN_2-as-mill sample as a function of heating time. The decrease in linewidth is because the corresponding linewidth for the free gaseous molecules are intrinsically much narrower than the surface adsorbed species. Similar trend is observed for the $LiNH_2$ + LiH-RT-180Min-mill sample. However, the half linewidth of the 4.1 ppm peak associated with the $LiNH_2$ + LiH-RT-180Min-mill sample is much larger, ranging from ~400 Hz (Fig. 4(a2)) to ~340 Hz (Fig. 4(d2)), indicating that the dominant H_2 molecules are surface adsorbed species over the entire heating period studied. It is known from Fig. 4 that for the sample of $LiNH_2$ + LiH ball milled at liquid nitrogen temperature for 180 min ($LiNH_2$-LiH-LN_2-as-mill), the amount of hydrogen rapidly accumulates during the 488 s heating period, from the initial 6.7% (Fig. 4(a1)) to 19.2% (Fig. 4(d1)). On the other hand, there is essentially no hydrogen release in the corresponding spectrum of $LiNH_2$ + LiH ball milled at room temperature for 180 min (Fig. 4(a2)), where only a very broad peak related to the hydrogen atoms in the rigid lattice was observed. Although the amount of H_2 accumulates with increasing time and temperature (Fig. 4(a2)–(d2)), the relative ratio of H_2 to the total protons in the sample is much lower than that of the liquid nitrogen milled mixture. For example, the amount of H_2 released is only about 4.1% (Fig. 4(d2)) of the total hydrogen atoms in the sample, whereas

about 19.2% H_2 was observed in Fig. 4(d1). These results reveal that the liquid nitrogen ball milled sample can release hydrogen faster than the room temperature ball milled sample. Thus, high-energy ball milling under the liquid nitrogen milling condition is an efficient way of performing mechanical activation. This conclusion is entirely consistent with the findings discussed in Section 3.2, where it is shown that ball milling at liquid nitrogen temperature results in more upfield shifting of the ^{6}Li peak at 2.7 ppm and a higher intensity of the 18–2.0 ppm peak than ball milling at room temperature.

4. Conclusions

It is demonstrated in this work that significantly enhanced spectral resolution is obtained in the ^{6}Li MAS NMR spectra of Li–N–H systems at ultra-high field of 21.1 T relative to that of the 7.05 T field used in the previous report [5]. The resolution enhancement is roughly proportional to the magnetic field strength, consistent with theoretical predictions when the line broadening mechanisms are mainly from the second-order quadrupole interaction. The significantly enhanced spectral resolution at ultra-high field is exploited to study the detailed electronic and chemical environment changes associated with mechanical activation of Li–N–H systems using high-energy balling milling. The effects of ball milling at both room temperature and liquid nitrogen temperature are compared. Furthermore, the hydrogen release dynamics in the ball-milled samples are investigated using *in situ* ^{1}H MAS NMR.

Major findings are summarized below. (a) High-energy ball milling causes an upfield shift of the resonances in ^{6}Li MAS spectra for all the samples studied. The upfield peak shift indicates changes in the average local electronic structure around Li nuclei through an increased electronic shielding. (b) In the mechanically activated mixture of $LiNH_2$ + LiH, a new peak centered about 2.0 ppm is observed, suggesting that high-energy ball milling has induced molecular interaction between $LiNH_2$ and LiH molecules. The intensity of the new peak increases with an increase in the milling time and a decrease in the milling temperature. The formation of this new peak has been attributed to significantly increased lattice defects on the surface of $LiNH_2$ and LiH particles induced by ball milling. (c) Ball milling at liquid nitrogen temperature is more efficient in mechanical activation than ball milling at room temperature based on the detailed spectral features in ^{6}Li MAS spectra and the speed of hydrogen released at comparable temperatures. (d) LiOH and $LiOH^{\bullet}H_2O$ resonant peaks have been separated from LiH and $LiNH_2$ resonant peaks, and are observed in both the as-purchased LiH and $LiNH_2$ samples. (e) In the fully discharged $LiNH_2$ + LiH system, the Li_2NH peak is observed at about 3.1 ppm.

Acknowledgements

This work was supported under the U.S. Department of Energy (DOE) Contract No. DE-FC36-05GO15008. The vision and support of Dr. Ned T. Stetson, DOE Technology Manager, are greatly appreciated. The research was performed in the Environmental Molecular Sciences Laboratory (a national scientific user facility sponsored by the Department of Energy's Office of Biological and Environmental Research) located at PNNL, and operated for DOE by Battelle under Contract No. DE-AC05-76RL01830.

References

[1] Z. Gan, P. Gor'kov, T.A. Cross, A. Samoson, D. Massiot, J. Am. Chem. Soc. 124 (2002) 5634–5635.
[2] A. Ortiz, W. Osborn, T. Markmaitree, L. Shaw, Crystallite sizes of LiH before and after ball milling and thermal exposure, J. Alloys Compd. 454 (2008) 297–305.
[3] W. Luo, S. Sickafoose, J. Alloys Compd. 407 (2006) 274–281.
[4] Z. Xiong, J. Hu, G. Wu, P. Chen, W. Luo, K. Gross, J. Wang, J. Alloys Compd. 398 (2005) 235–239.
[5] C. Lu, J.Z. Hu, J.H. Kwak, Z. Yang, R. Ren, T. Markmaitree, L.L. Shaw, J. Power Sources 170 (2007) 419–424.
[6] P. Chen, Z. Xiong, J.Z. Luo, J.Y. Lin, K.L. Tan, Nature 420 (2002) 302–304.
[7] P. Chen, Z. Xiong, J.Z. Luo, J.Y. Lin, K.L. Tan, J. Phys. Chem. B 107 (2003) 10967–10970.
[8] Y.H. Hu, E. Ruckenstein, Ind. Eng. Chem. Res. 42 (2003) 5135–5139.
[9] Y.H. Hu, E. Ruckenstein, J. Phys. Chem. A 107 (2003) 9737–9739.
[10] T. Ichikawa, N. Hanada, S. Isobe, H. Leng, H. Fujii, J. Phys. Chem. B 108 (2004) 7887–7892.
[11] T. Ichikawa, S. Isobe, N. Hanada, H. Fujii, J. Alloys Compd. 365 (2004) 271–276.
[12] S. Orimo, Y. Nakamori, G. Kitahara, K. Miwa, N. Ohba, T. Noritake, S. Towata, Appl. Phys. A 79 (2004) 1765–1767.
[13] T. Ichikawa, N. Hanada, S. Isobe, H. Leng, H. Fujii, Mater. Trans. 46 (2005) 1–14.
[14] Y. Kojima, Y. Kawai, J. Alloys Compd. 395 (2005) 236–239.
[15] Y.H. Hu, E. Ruckenstein, Ind. Eng. Chem. Res. 43 (2004) 2464–2467.
[16] J.H. Yao, C. Shang, K.F. Aguey-Zinsou, Z.X. Guo, J. Alloys Compd. 432 (2007) 277–282.
[17] H.Y. Leng, T. Ichikawa, S. Isobe, S. Hino, N. Hanada, H. Fujii, J. Alloys Compd. 404–406 (2005) 443–447.
[18] G.P. Meisner, F.E. Pinkerton, M.S. Meyer, M.P. Balogh, M.D. Kundrat, J. Alloys Compd. 404–406 (2005) 24–26.
[19] S. Isobe, T. Ichikawa, N. Hanada, H.Y. Leng, M. Fichtner, O. Fuhr, H. Fujii, J. Alloys Compd. 404–406 (2005) 439–442.
[20] T. Ichikawa, N. Hanada, S. Isobe, H.Y. Leng, H. Fujii, J. Alloys Compd. 404–406 (2005) 435–438.
[21] L.L. Shaw, R. Ren, T. Markmaitree, W. Osborn, J. Alloys Compd. 448 (2008) 263–271.
[22] T. Markmaitree, R. Ren, L.L. Shaw, J. Phys. Chem. B 110 (2006) 20710–20817.
[23] Z.G. Yang, L. Shaw, Nanostruct. Mater. 7 (1996) 873–886.
[24] R. Ren, A.L. Ortiz, T. Markmaitree, W. Osborn, L. Shaw, J. Phys. Chem. B 110 (2006) 10567–10575.
[25] W. Osborn, T. Markmaitree, L. Shaw, J. Power Sources 172 (2007) 376–378.
[26] B.M. Meyer, N. Leifer, S. Sakamoto, S.G. Greenbaum, C.P. Grey, Electrochem. Solid-State Lett. 8 (2005) A145–A148.
[27] K.D.J. Mackenzie, M.E. Smith, Multinuclear Solid Solid-State NMR of Inorganic Materials. Pergamon Materials Series, Pergamon, An Imprint of Elsevier Science, New York, 2002.
[28] M. Wilkening, C. Mulhle, M. Jansen, P. Heitjans, J. Phys. Chem. B 111 (2007) 8691–8694.